JB
Journals.ASM.org

Staphylococcus epidermidis agr Quorum-Sensing System: Signal Identification, Cross Talk, and Importance in Colonization

Michael E. Olson,[a] Daniel A. Todd,[b] Carolyn R. Schaeffer,[c] Alexandra E. Paharik,[a] Michael J. Van Dyke,[a] Henning Büttner,[e] Paul M. Dunman,[d] Holger Rohde,[e] Nadja B. Cech,[b] Paul D. Fey,[c] Alexander R. Horswill[a]

Department of Microbiology, Roy J. and Lucille A. Carver College of Medicine, University of Iowa, Iowa City, Iowa, USA[a]; Department of Chemistry and Biochemistry, University of North Carolina Greensboro, Greensboro, North Carolina, USA[b]; Department of Pathology and Microbiology, University of Nebraska Medical Center, Omaha, Nebraska, USA[c]; Department of Microbiology and Immunology, University of Rochester Medical Center, Rochester, New York, USA[d]; Institute for Medical Microbiology, Virology and Hygiene, University Medical Centre Hamburg-Eppendorf, Hamburg, Germany[e]

Staphylococcus epidermidis **is an opportunistic pathogen that is one of the leading causes of medical device infections. Global regulators like the *agr* quorum-sensing system in this pathogen have received a limited amount of attention, leaving important questions unanswered. There are three *agr* types in *S. epidermidis* strains, but only one of the autoinducing peptide (AIP) signals has been identified (AIP-I), and cross talk between *agr* systems has not been tested. We structurally characterized all three AIP types using mass spectrometry and discovered that the AIP-II and AIP-III signals are 12 residues in length, making them the largest staphylococcal AIPs identified to date. *S. epidermidis agr* reporter strains were developed for each system, and we determined that cross-inhibitory interactions occur between the *agr* type I and II systems and between the *agr* type I and III systems. In contrast, no cross talk was observed between the type II and III systems. To further understand the outputs of the *S. epidermidis agr* system, an RNAIII mutant was constructed, and microarray studies revealed that exoenzymes (Ecp protease and Geh lipase) and low-molecular-weight toxins were downregulated in the mutant. Follow-up analysis of Ecp confirmed the RNAIII is required to induce protease activity and that *agr* cross talk modulates Ecp activity in a manner that mirrors the *agr* reporter results. Finally, we demonstrated that the *agr* system enhances skin colonization by *S. epidermidis* using a porcine model. This work expands our knowledge of *S. epidermidis agr* system function and will aid future studies on cell-cell communication in this important opportunistic pathogen.**

Staphylococcus epidermidis is a human commensal of the skin and mucosal surfaces and is one of the best-known members of the coagulase-negative staphylococci (CoNS) (1). CoNS are the most frequent cause of hospital-associated infections (HAIs) (2), including central-line-associated infections, and the second most common cause of surgical-site infections and prosthetic-valve infective endocarditis (3). Over 150 million intravascular devices are used each year in the United States alone (4), and a major risk factor for CoNS disease is the presence of a medical implant (5). For many of these infections, *S. epidermidis* makes up more than 80% of the clinical burden of CoNS (3, 6).

The ability of *S. epidermidis* to colonize implanted devices and form a biofilm is its primary mechanism of pathogenesis (1, 6). The polysaccharide intercellular adhesin (PIA) produced by proteins encoded in the *icaADBC* locus is one of the best-characterized biofilm determinants (7). More recently, protein-mediated biofilm mechanisms have been identified (reviewed in reference 6), with the accumulation-associated protein (Aap) being one of the best studied (8). Regulation of biofilm formation has been a focus of numerous studies, and some of these investigations have demonstrated that the *agr* quorum-sensing system impacts *S. epidermidis* biofilm development. In this regard, strains defective in *agr* have been shown to display enhanced adherence and biofilm properties (9, 10) and reduced production of extracellular enzymes, such as lipases and proteases (10–12). The *agr*-regulated low-molecular-weight toxins, termed phenol-soluble modulins (PSMβs), are known to disrupt *S. epidermidis* biofilms and to be important for dissemination during biofilm infection (13).

The fundamental features of the *agr* system are conserved in a number of staphylococcal species, including *S. epidermidis* (14). Each of these systems is controlled by an extracellular peptide signal called an autoinducing peptide (AIP), which is secreted during growth and activates gene expression in a cell density-dependent manner. Among the staphylococci, the AIPs are typically 7 to 9 amino acids in length, and the last five residues are cyclized into a lactone or thiolactone structure through a serine or cysteine side chain, respectively. Much of the knowledge on the mechanistic details of the *agr* system is based on studies carried out with *Staphylococcus aureus* (reviewed in references 14 and 15). Briefly, the *agr* locus is composed of the *agrBDCA* operon, which encodes the core machinery for producing and detecting AIPs (Fig. 1). AgrD serves as the propeptide precursor that is secreted and processed by AgrB, a multipass integral membrane peptidase that works with signal peptidase SpsB to secrete AIP. Accumulation of extracellular AIP is detected by the histidine kinase AgrC. When AIP binds to this receptor, a signal transduction cascade is initiated, with AgrC phosphorylating the response regulator AgrA, resulting in induction of expression from the *agr* P_2 and P_3 promoters (Fig. 1), as well as the promoters controlling expression of PSM transcripts. The P_3 promoter drives the expression of the transcript RNAIII, which is the primary effector of the system.

Received 25 May 2014 **Accepted** 18 July 2014
Published ahead of print 28 July 2014
Address correspondence to Alexander R. Horswill, alex-horswill@uiowa.edu.
M.E.O. and D.A.T. contributed equally to this work.

doi:10.1128/JB.01882-14

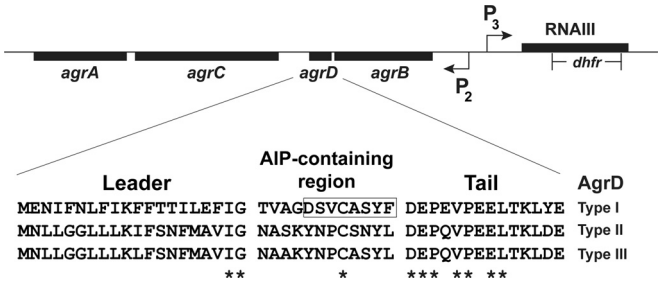

FIG 1 Schematic of the staphylococcal *agr* locus and *S. epidermidis* AgrD sequences. The three AgrD types are shown and are divided into the leader region, AIP-containing region, and tail region. The highly conserved residues across staphylococcal AgrDs are indicated by asterisks. The previously deduced AIP-I structure is boxed. Also diagramed is the deletion/insertion of the *dhfr* cassette that disrupts RNAIII in *S. epidermidis* 1457 to yield the Δ*rnaIII*::*dhfr* mutant used in this study.

There remain important unanswered questions about the *S. epidermidis agr* system. Following the initial description of the locus (16, 17), it was several years before sequencing studies revealed three different classes of *S. epidermidis agr* systems in clinical isolates (18), which are referred to here as *agr* types I, II, and III. Although there has been some effort to correlate these classes with *S. epidermidis* disease (19–23), the presence of different *agr* classes, and their unique AIP signals, has remained largely overlooked. Of these, only the AIP-I structure has been characterized (16). Many studies have focused on prototype biofilm-forming strain 1457, which encodes an *agr* type II system, but the structure of *S. epidermidis* AIP-II is not known.

Our goal in this study was to gain a better understanding of *S. epidermidis agr* system function and address several open questions. By using bioactivity-guided fractionation and high-resolution mass spectrometry, the AIP signal structures were determined and cross talk between each of *S. epidermidis agr* systems was investigated. An RNAIII mutant was constructed in strain 1457; the regulatory changes in this mutant were assessed, and a skin colonization phenotype was identified. Collectively, these results provide new insights into the molecular details, function, and importance of the *S. epidermidis agr* system.

MATERIALS AND METHODS

Growth conditions and reagents. Bacterial strains used in this study are listed in Table 1. *Escherichia coli* was grown in LB medium, and *S. epidermidis* cultures were grown in tryptic soy broth (TSB). *S. epidermidis* cultures were grown at 37°C with the appropriate antibiotics at concentrations of 10 μg/ml for chloramphenicol (Cam), erythromycin (Erm), and trimethoprim (Tmp) and 50 μg/ml for kanamycin (Kan), as needed. Chemical reagents were purchased from Sigma-Aldrich (St. Louis, MO) unless otherwise noted. *S. epidermidis* AIP-II was custom synthesized by American Peptide Company (Vista, CA). All oligonucleotides used in this study are listed in Table 2.

Strain and plasmid constructions. Plasmid constructions were performed in *E. coli* using standard techniques. DNA sequencing was performed at the University of Nebraska Medical Center (UNMC) core sequencing laboratory. Following passage through the restriction-deficient *S. aureus* strain RN4220 (24), plasmid DNA was electroporated into *S. epidermidis* strains as previously described (25). Plasmids were moved between *S. epidermidis* strains using bacteriophage 71 transduction as previously described (26).

Construction of an RNAIII mutant. The RNAIII allelic replacement vector (pNF41) was designed to have two regions of sequence similarity to the *S. epidermidis* chromosome flanking the dihydrofolate reductase (*dhfr*) gene from plasmid pGO558 (27), which confers resistance to Tmp. The first fragment was a 697-bp piece of the 5′ region of RNAIII that was PCR amplified from *S. epidermidis* RP62A using oligonucleotides 367 and 378 (Table 2). The PCR product was digested with EcoRI and BamHI and was ligated into pUC19 cut with the same enzymes. The second fragment was a 991-bp 3′ region of RNAIII amplified from *S. epidermidis* RP62A with primers 369 and 379, and this PCR product was digested with SalI and PstI and cloned into the same sites on the pUC19-5′-RNAIII plasmid. The *dhfr* gene was excised from pGO558 with a SalI digest and was ligated into the same site on the RNAIII knockout plasmid to provide Tmp resistance. Finally, pROJ6448 (28) was linearized with PstI and inserted into the plasmid to provide a temperature-sensitive staphylococcal replicon and Erm resistance.

Construction of an *ecp* mutant. Roughly 1,000-bp regions flanking the *ecp* gene were amplified from chromosomal *S. epidermidis* 1457 DNA using primers Ecp5_att_for, Ecprev_Eco, 3_for_Eco, and Ecp_att_rev3 (Table 2). Amplicons were purified, cleaved using EcoRI, and ligated by T4 ligase. The 2,000-bp ligation product was cloned into pKOR1 using the BP Clonase reaction (Invitrogen), resulting in pKO*ecp*. pKO*ecp* was introduced into *S. aureus* RN4220 by electroporation and, from there, again by electroporation into *S. epidermidis* mutant 1457-M12 (29). Using phage A6C, pKO*ecp* was next transduced into *S. epidermidis* 1457 (8). Allelic replacement was carried out essentially as described previously (30). Putative mutants were screened by PCR, and the loss of *ecp* was verified by sequence analysis.

TABLE 1 Strains and plasmids

Strain or plasmid	Description	Source or reference
E. coli DH5α	Cloning strain	New England Biolabs
S. aureus		
AH1263	LAC Erm^s	52
RN4220	Restriction deficient strain	24
S. epidermidis		
ATCC 12228	Clinical isolate (*ica agr* type I)	53
1457 (AH2490)	Clinical isolate (*ica*$^+$ *agr* type II)	54
RP62a	Clinical isolate (*ica*$^+$ *agr* type I)	55
4804	Clinical isolate (*agr* type I)	Fey collection
7237	Clinical isolate (*agr* type I)	Fey collection
5183	Clinical isolate (*agr* type II)	Fey collection
7022	Clinical isolate (*agr* type II)	Fey collection
8595	Clinical isolate (*agr* type II)	Fey collection
8099	Clinical isolate (*agr* type III)	Fey collection
5794	Clinical isolate (*agr* type III)	Fey collection
8247	Clinical isolate (*agr* type III)	Fey collection
AH2673	1457/pCM40 (Erm^r)	This work
AH2491	1457 Δ*rnaIII*::*dhfr*	This work
AH2589	1457 Δ*ica*::*dhfr*	27
AH2924	1457 Δ*ecp*	This work
AH3408	ATCC 12228/pCM40 (Erm^r)	This work
AH3409	8247/pCM40 (Erm^r)	This work
Plasmids		
pCM11	P_{sarA}-sGFP Erm^r	50
pCM40	*agr* P3-sGFP Erm^r	This work
pGO558	Source of *dhfr* cassette; Tmp^r	27
pKOR1	Knockout vector	30
pROJ6448	Temp-sensitive replicon	28
pUC19	Cloning vector	New England Biolabs

TABLE 2 Oligonucleotides used in this study

Name	Sequence
367 (3′ *rnaIII*-F)	GGAATTCCCGACTAATGCCATAGATAAAAG
378 (3′ *rnaIII*-R)	CGGGATCCCACCGATTGTAGAAATGATATC
369 (5′ *rnaIII*-F)	ACGCGTCGACGCCGTGAGTCTCTCCCAAG
379 (5′ *rnaIII*-R)	AACTGCAGGTAACTAAAGCTTTACCCTAAGC
ARH132	GTTGTTAAGCTTCTGTCATTATACGATTTAGTACAATC
ARH133	GTTGTTGGTACCTTAAACAACTCATCAACTATTTTCC
2298 (*ecp*-F)	TGTGCTTAAAACGCCACGTA
2299 (*ecp*-R)	GTATAGCCGGCACACCAACT
2301 (*gyrB*-F)	CTCGAAGCGGTTCGTAAAAG
2302 (*gyrB*-R)	TACCACGGCCATTGTCAGTA
2547 SERP0736 (*psmβ1*)-F	CGGCCTCATTTAGGAGTG
2548 SERP0736 (*psmβ1*)-R	CGATTCACCATATCAACGC
Ecp5_att_for	GGGGACAAGTTTGTACAAAAAAGCAGGCTTAGCGTGGTGAAGTTAATGATG
Ecprev_Eco	CAACACATGAATTCGCTAGCTTTTGCAACTCTTTCAAATCG
3_for_Eco	CAACACATGAATTCGCGGCCGCTATTAATATAGAAAGGTGTGCTTATGC
Ecp_att_rev3	GGGGACCACTTTGTACAAGAAAGCTGGGTAGAAGATATTCATATTAGTGGTGCTG

Construction of *S. epidermidis agr* reporter strains. The *agr* P3 promoter was PCR amplified from *S. aureus* strain AH1263 using oligonucleotides ARH132 and ARH133 (Table 2). The PCR product was digested with HindIII and KpnI and cloned into the same sites on plasmid pCM11. The new plasmid was confirmed for *agr* responsiveness and called pCM40. Plasmid pCM40 was transformed into *S. epidermidis* 1457 to construct reporter strain AH2673. The reporter plasmid was transduced to other strains using bacteriophage 71 to construct AH3408 and AH3409 reporters.

***agr* P3-sGFP reporter assays.** For the *agr* P3-sGFP time course, an overnight culture of reporter strain AH2673 was diluted to an optical density at 600 nm (OD_{600}) of 0.05 in 20 ml of TSB in 125-ml flasks supplemented with 10 μg/ml Erm. For exogenous AIP-II addition, spent medium was collected from *S. epidermidis* 1457 by centrifuging 24-h cultures at 3,750 rpm and filtering through 0.22-μm filters. The spent medium was added to the reporter culture at a final concentration of 10% (vol/vol). Cultures were grown at 37°C with shaking (250 rpm). Measurements of the optical density at 600 nm (OD_{600}) and superfolder green fluorescent protein (sGFP) fluorescence (excitation, 490 nm; emission, 520 nm) were obtained hourly for 27 h using a Tecan Infinite M200 plate reader. For each measurement, 3 samples of 200 μl were removed from each flask and transferred to a 96-well microtiter plate (Corning 3096). The values are reported as relative fluorescence after normalization to OD_{600} readings. At least three biological replicates were performed for each condition. Of note, the AH2673 reporter strain was reconstructed for the time course.

For the cross talk tests, *S. epidermidis* strains representing different *agr* systems were grown for 20 h in TSB, and spent medium was collected and passed through 0.22-μm filters. The *agr* reporters for type I (AH3408), type II (AH2673), and type III (AH3409) were grown overnight in 5 ml of TSB with Erm and subcultured 1:200 into 18-mm tubes with fresh culture medium. The filtered spent medium collected from *S. epidermidis* strains was added to 10% (vol/vol). The reporter cultures were grown for 24 h, and growth (OD_{600}) and sGFP measurements were obtained as described above.

Transcriptional profiling. Overnight cultures of *S. epidermidis* 1457 and 1457 Δ*rnaIII*::*dhfr* were diluted 1:100 into fresh TSB and grown at 37°C to an OD_{600} of 8.2 (flask-to-volume ratio, 5:1; shaking at 200 rpm). RNA was converted to cDNA, and microarray analysis was performed according to the manufacturer's instructions (Affymetrix expression analysis technical manual; Affymetrix, Inc., Santa Clara, CA) for antisense prokaryotic arrays as described previously by Beenken and colleagues (31). To ensure reproducibility, cDNA samples from each strain were prepared from two separate experiments. Each cDNA sample was hybridized to an *S. epidermidis* GeneChip. Signal intensity values for each qualifier (predicted open reading frame [ORF] and intergenic region) were normalized to the median signal intensity value for each GeneChip. Sample values were then averaged. Genes for which there was at least a 2-fold difference ($P \leq 0.05$, *t* test) in RNA titer between 1457 and 1457 Δ*rnaIII*::*dhfr* were considered differentially expressed in an *rnaIII*-dependent manner.

δ-Toxin immunoblots. For the δ-toxin immunoblots, strain 1457, strain 1457 supplemented with 40 nM AIP-II, and the 1457 Δ*rnaIII*::*dhfr* mutant were grown in TSB for 21 or 24 h at 37°C. Cells were removed by filtration through 0.22-μm filters, and spent medium was used for the immunoblots. Immunoblotting for δ-toxin was performed by cross-reactivity with rabbit polyclonal antisera to *S. aureus* δ-toxin (Abgent, San Diego, CA), diluted 1:1000, followed by secondary goat anti-rabbit IgG (1:1,000) conjugated to horseradish peroxidase (Toxin Technology, Sarasota, FL) as previously described (32).

Ecp activity analysis. A protease assay was developed to follow Ecp activity using FRET substrate [5-carboxyfluorescein (FAM)-Lys-Leu-Leu-Asp-Ala-Ala-Pro-(QXL520)-OH; AnaSpec, Fremont, CA]. This substrate is based on the CXCR2 substrate developed for *S. aureus* staphopain A (33), and it was suspended to 50 μM using 20 mM Tris (pH 7.4). For Ecp activity analysis, strains were grown in TSB for 12 h at 37°C. Cells were removed by filtration through 0.22-μm filters, and spent medium was saved for the analysis. A 50-μl portion of collected medium was mixed with 25 μl of the FRET substrate in a microtiter plate, and fluorescence measurements (excitation, 490 nm; emission, 520 nm) were obtained at 37°C in a Tecan Infinite M200 plate reader. Reaction rates were recorded as units of fluorescence per minute.

For the *agr* cross talk impact on Ecp activity, spent medium from different *S. epidermidis* strains was prepared as described above for the *agr* reporter methods. For the Ecp measurements, cultures were prepared as described above except that collected spent medium was added to 10% (vol/vol) of the testing strain at the time of inoculation. Finally, cells were removed, and Ecp activity was measured in the samples.

Reverse transcriptase PCR. Overnight cultures were diluted 1:100 and grown microaerobically (5:1 [vol/vol], flask-to-medium ratio) in TSB to an OD_{600} of ~7.6. Samples were spun at 6,000 × *g* for 5 min at 4°C. Pellets were resuspended in RLT buffer (Qiagen) with 0.01% β-mercaptoethanol. Cells were lysed by mechanical disruption and the cell debris was removed by centrifugation at 21,000 × *g* for 15 min at 4°C. The supernatant was removed to a new tube with 0.7 volume of ethanol and vortexed. RNA was prepared using the RNeasy kit (Qiagen) according to the manufacturer's instructions. cDNA was synthesized from approximately 1.5 μg of RNA using the Transcriptor first-strand cDNA synthesis

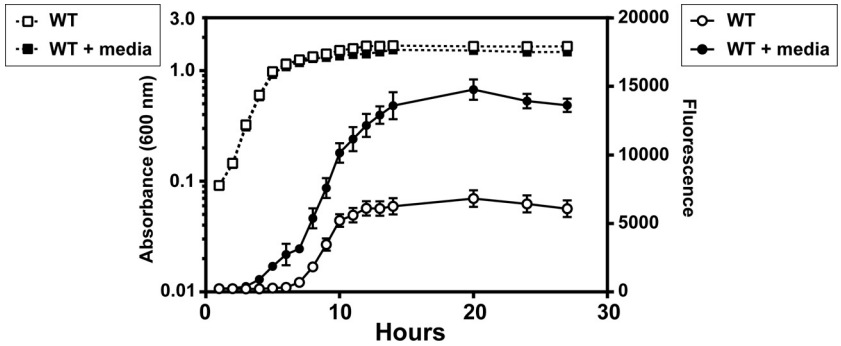

FIG 2 Development of *agr* reporters for *S. epidermidis* 1457. Plasmid pCM40 (*agr* P_3-GFP) was transformed into WT 1457, and reporter strains were grown in TSB (open symbols) or TSB with spent medium added to 10% of total volume (filled symbols). Absorbance (dashed lines) and fluorescence (solid lines) readings were taken at the indicated points throughout the time course.

kit (Roche) according to the manufacturer's instructions using the random hexamer primer. RT-PCR mixtures contained Quik-Load 2× Midas PCR mix (Monserate Biotech, San Diego, CA), 10 μM primers, and 2 μl of cDNA. Reactions were run in a MyCycler thermocycler (Bio-Rad) for 20 cycles with a 15-s extension. Following agarose gel electrophoresis, DNA bands were visualized by ethidium bromide staining.

Fractionation of *S. epidermidis* spent medium. *S. epidermidis* strain 5183 was grown in TSB at 37°C with shaking at 200 rpm overnight. Cells were pelleted by centrifugation at 6,000 × *g* for 5 min. and removed by 0.22-μm filtration. The filtered medium was separated by automated flash chromatography using a Teledyne Isco Combiflash Rf system. A RediSep Rf Gold C_{18} column was used with a linear methanol-water gradient starting at 10% methanol and ending at 100% methanol over 100 column volumes, and the fractions were collected in 25-ml test tubes.

LC-MS identification and quantification of S. epidermidis AIP. All liquid chromatography-mass spectrometry (LC-MS) analyses were performed on a Waters Acquity ultraperformance liquid chromatograph (UPLC) coupled to a Thermo Fisher Scientific LTQ Orbitrap XL mass spectrometer with electrospray source. Samples (5 μl) were injected onto a high-strength silica (HSS) T3 C_{18} column (Waters Corporation). Analyses were conducted at a flow rate of 0.250 ml/min with the following binary gradient, where solvent A is 0.1% formic acid in H_2O, and solvent B is 0.1% formic acid in acetonitrile: 0 to 6 min, from 80% A to 20% A; 6.0 to 6.5 min, from 20% A to 80% A; 6.5 to 7.0 min, 80% A (isocratic).

Analyses were conducted in both the positive- and negative-ion modes. In positive-ion mode, the Orbitrap was operated at a scan range of *m/z* 300 to 2,000 with the following settings: tube lens voltage, 110 V; source voltage, 4.50 kV; source current, 100 μA; heated-capillary voltage, 20.0 V; heated-capillary temperature, 300.0°C; sheath gas flow rate, 20.0; auxiliary gas flow rate, 0. For negative-ion mode analyses, the Orbitrap was operated at a scan range of *m/z* 300 to 2,000 with the following settings: tube lens voltage, 100 V; source voltage 4.00 kV; source current, 100 μA; heated-capillary voltage, 20.0 V; heated-capillary temperature, 275.0°C; sheath gas flow rate, 25.0; auxiliary gas flow rate, 0. For MS-MS analysis in the negative-ion mode, the precursor masses of 873.34, 1,355.60, and 1296.60 (the predicted masses of deprotonated AIP-I, AIP-II, and AIP-III, respectively) were subjected to collision-induced dissociation with activation energy of 35%. The same MS-MS conditions were used in the positive ion mode, but precursor *m/z* values for protonated AIP-I, API-II, and AIP-III (873.34, 1,355.60, and 1,296.60, respectively) were selected.

The AIP-II concentration was calculated using an 8-point calibration curve of synthetic AIP-II ranging in concentration from 30.0 μM to 0.3 μM by 2-fold dilutions. The calibration curve was generated by plotting log(peak area) versus log(concentration). Peak area was selected for a *m/z* of 678.38 (the most intense product peak for mass 1,355.60) from the MS-MS selected ion chromatogram. AIP-II concentrations were calculated using the slope of the best-fit line obtained by linear regression analysis of the calibration curve data.

***S. epidermidis* colonization of porcine skin.** *S. epidermidis* colonization of porcine skin was performed as described previously (34). Biopsy punches of 8 mm were taken from the ears of newborn piglets (tissue kindly provided by D. Stoltz). Explanted tissue was washed prior to biopsy with ethanol, and biopsy punches were placed individually on a piece of sterile gauze in 12-well cell culture plates. The skin biopsy specimens were cultured in Dulbecco's modified Eagle medium (DMEM) containing hydrocortisone, 10% fetal bovine serum (FBS), and penicillin-streptomycin (35). The growth medium was added to the wells, bringing the height near the apical surface of the biopsy specimen. These samples were incubated at 37°C with 5% CO_2 for the duration of the experiment, and the culture medium was changed daily. After 15 h of incubation, 10 μl of bacterial suspension in saline containing 1.5×10^4 to 2×10^4 CFU of wild-type (WT) 1457 or 3.8×10^4 to 7.5×10^4 CFU of 1457 Δ*rnaIII*::*dhfr* was spotted on the apical skin surface. The cultures were allowed to dry onto the skin surface in a laminar flow hood for 1 h, and the plates were returned to the incubator. After 48 h of incubation, the skin biopsy specimen was placed in1 ml of phosphate-buffered saline (PBS) and vortexed at maximum speed for 1 min. The cells were serially diluted, plated on high-salt tryptic soy agar (TSA) (supplemented with 50 g/liter NaCl), incubated overnight at 37°C, and enumerated.

RESULTS

***S. epidermidis agr* systems.** *S. epidermidis* clinical isolates have any one of three classes of *agr* systems (Fig. 1) (18), and of these, only the structure and activity of the AIP-I signal have been characterized to date (16). We sought to expand this knowledge and define each of the three *S. epidermidis* AIP molecules. In particular, we focused on the unknown AIP-II structure found in prototype strain 1457 (*agr* type II system), which is one of the model strains for molecular genetic studies in *S. epidermidis*. To achieve this goal, we developed bioassay strains in the 1457 background that contained an *agr* P_3-sGFP reporter (pCM40) that responds to quorum-sensing activity in a manner similar to that of *S. aureus agr* reporters (36). As expected, the *S. epidermidis agr* system was activated, and sGFP accumulated over time (Fig. 2). The exogenous addition of 1457 spent medium containing AIP-II triggers a positive-feedback loop, causing an acceleration of the *agr* activation kinetics.

AIP identification. Using the new 1457 *agr* reporter strain, we tested various *S. epidermidis agr* type II isolates to enable selection of the most active strain for fractionation purposes. Clinical isolate 5183 was chosen as the best producer; spent medium from this

strain had the strongest enhancement of *agr* activation kinetics in the reporter assay. To characterize the signal, strain 5183 spent medium was fractionated by reverse-phase flash chromatography. Fractions were tested for their influence on the 1457 *agr* reporter, and one fraction was identified that enhanced reporter output (data not shown). The AgrD type II sequence (Fig. 1) was used as a guide for predicting the *m/z* value of the type II molecular ion, starting with the predicted 8-residue sequence YNPCSNYL, which would represent a 5-residue cyclic thiolactone (CSNYL) and 3-residue amino-terminal extension. The masses that resulted from adding or removing amino-terminal residues were calculated, and the mass-spectral data were filtered to find an *m/z* value matching the exact mass (within 5 ppm) of a predicted peptide. Using this strategy, the peptide NASKYNPCSNYL (Fig. 3B), *m/z* 1353.5879 $[M\text{-}H]^-$ (calculated for $C_{59}H_{85}N_{16}O_{19}S^-$, 1,353.5903; 1.8 ppm mass accuracy), was detected. This finding suggested that AIP-II is a 12-residue peptide that contains a 5-residue cyclic thiolactone ring and a 7-residue amino terminal extension. As further support for this identification, strain 1457 was analyzed using the outlined method, and the same results were obtained (data not shown). The proposed 12-residue structure makes the *S. epidermidis* AIP-II the largest staphylococcal AIP identified to date.

The AIP identification approach described for *S. epidermidis* AIP-II was also applied to the other *S. epidermidis agr* systems. For the *agr* type I system, the clinical isolate 4804 was tested, and an ion matching the peptide DSVCASYF, *m/z* 873.3453 $[M+H]^+$ (calculated for $C_{39}H_{53}N_8O_{13}S^+$, 873.3447; 0.8 ppm mass accuracy), was detected (Fig. 3A). This is consistent for the sequence previously proposed for *S. epidermidis* AIP-I (16). For the *agr* type III system, we tested clinical isolate 5794 and detected an ion at *m/z* 1,296.6011, consistent with the predicted mass of the protonated form of the peptide NAAKYNPCASYL (measured, 1,296.6011; calculated for $C_{58}H_{86}N_{15}O_{17}S^+$, 1,296.6041; 2.3 ppm mass accuracy) (Fig. 3C). AIP-III likewise is an unusually large structure, similar in size to the AIP peptide detected in the spent medium of *S. epidermidis* AIP-II.

To confirm the AIP identification, the proposed AIP-II peptide was synthesized and used in verification studies. The retention time (Fig. 4A) and MS-MS fragmentation pattern (Fig. 4C) of synthetic AIP-II matched those of the putative AIP-II ion from *S. epidermidis* AIP-II strains (Fig. 4B and D). Synthetic AIP-II was also used to quantify the levels of AIP-II in the spent medium, and it was determined that strain 1457 produced 1 μM AIP-II in stationary phase after 19 h of growth in TSB. Finally, the synthetic AIP-II was added to the 1457 *agr* reporter strain, and it accelerated activation kinetics in a manner that mirrored those in 1457 spent medium (Fig. 4E), indicating that the proposed AIP-II structure is functional. Collectively, the data presented in this section demonstrate that the fractionation-and-MS approach was effective for accurately identifying the biologically active AIP signals from *S. epidermidis*.

***S. epidermidis agr* cross talk.** Considering the large size of AIP-II and AIP-III (12 residues) versus the smaller AIP-I (8 residues), we reasoned that *agr* cross talk between *S. epidermidis* strains might occur, as has been observed with *S. aureus* (37). To evaluate this, *agr* reporters in type I and III strains were constructed and validated, similar to what was done with the type II strain (Fig. 2). To assess interference, spent medium from selected *agr* type I, II, and III strains was collected and added to cultures of the *agr* type I reporter (Fig. 5A), type II reporter (Fig. 5B), and type III reporter (Fig. 5C). In *agr* type I, the addition of spent medium containing AIP-I minimally enhanced output, while the addition of AIP-II or AIP-III markedly repressed GFP production (Fig. 5A). The weak positive feedback from the cognate signal is not unusual. The closely related *S. aureus agr* system does not respond strongly to exogenous signal addition unless specific growth conditions are used (38). In *S. epidermidis agr* type II, the addition of spent medium containing AIP-II significantly enhanced output, supporting our previous observations (Fig. 2), while AIP-I repressed GFP production (Fig. 5B). Interestingly, AIP-III neither enhanced nor repressed *agr* output. In *agr* type III, similar observations were made, with spent medium containing AIP-III enhancing GFP expression (Fig. 5C), and the medium containing AIP-I inhibiting it. The AIP-II signal had no significant impact on the *agr* type III reporter. Taken together, these data demonstrate that *agr* interference does occur among *S. epidermidis* strains. Specifically, interference occurs between the *agr* type I and II/III systems but not between the type II and III systems (Fig. 5D).

***S. epidermidis agr* mutant profiling.** To assess the regulatory profile of the *agr* system in *S. epidermidis*, an RNAIII allelic replacement mutant was constructed in strain 1457 (the region replaced with the *dhfr* cassette is shown in Fig. 1). Microarray transcriptional profiling was performed on the Δ*rnaIII*::*dhfr* mutant and revealed 21 genes that were downregulated compared to the WT (Fig. 6A). These results included δ-toxin, which was expected given that this toxin is encoded in the RNAIII transcript. The PSMβ, *agrC*, and *geh* genes were also identified as being downregulated, confirming a previous study that demonstrated the expression of these genes to be *agr* dependent (11). The cysteine proteinase, Ecp, was identified as one of the most significantly regulated genes (19-fold reduction in the mutant), which is also in line with previous studies (11). The staphostatin EcpB, which is encoded in a dicistronic operon with Ecp, showed a similar level of downregulation (Fig. 6A).

Subsequent to AIP identification, we sought to confirm some of the regulatory observations from the transcriptional profiling using reverse transcriptase PCR (RT-PCR) and exogenous addition of synthetic AIP-II. The downregulation of the PSMβ and *ecp* transcripts was confirmed by using *gyrB* as a reference (Fig. 6B). For the signal addition experiment, 40 nM AIP-II was added to broth cultures of 1457, and medium was harvested at 21 and 24 h of growth. δ-Toxin accumulation in the medium was assessed by protein immunoblotting, and as anticipated, the addition of AIP-II to the medium led to increased production of δ-toxin (Fig. 6C). The Δ*rnaIII*::*dhfr* mutant, which does not produce δ-toxin, was included as a negative control.

***agr* regulation of the cysteine protease Ecp.** Based on our *ecp* regulatory findings, we analyzed Ecp activity to assess the impact of the *agr* system on the extracellular proteome. We recently developed assays for *S. aureus* staphopain A based on the CXCR2 receptor (33, 39), and we tested whether these assays could translate to *S. epidermidis*. 1457 spent medium containing Ecp cleaved the CXCR2 substrate (data not shown), and this activity was inhibited with E-64, as expected for this protease (40). We have adapted the CXCR2 cleavage substrate to a smaller FRET peptide (39), and 1457 spent medium containing Ecp also cleaved this substrate (Fig. 7A). In support of the transcriptional profiling, spent medium from the 1457 Δ*rnaIII*::*dhfr* mutant showed an 8.6-fold reduction in Ecp activity. As a control, a 1457 Δ*ecp* mutant was constructed, and this mutant did not possess activity

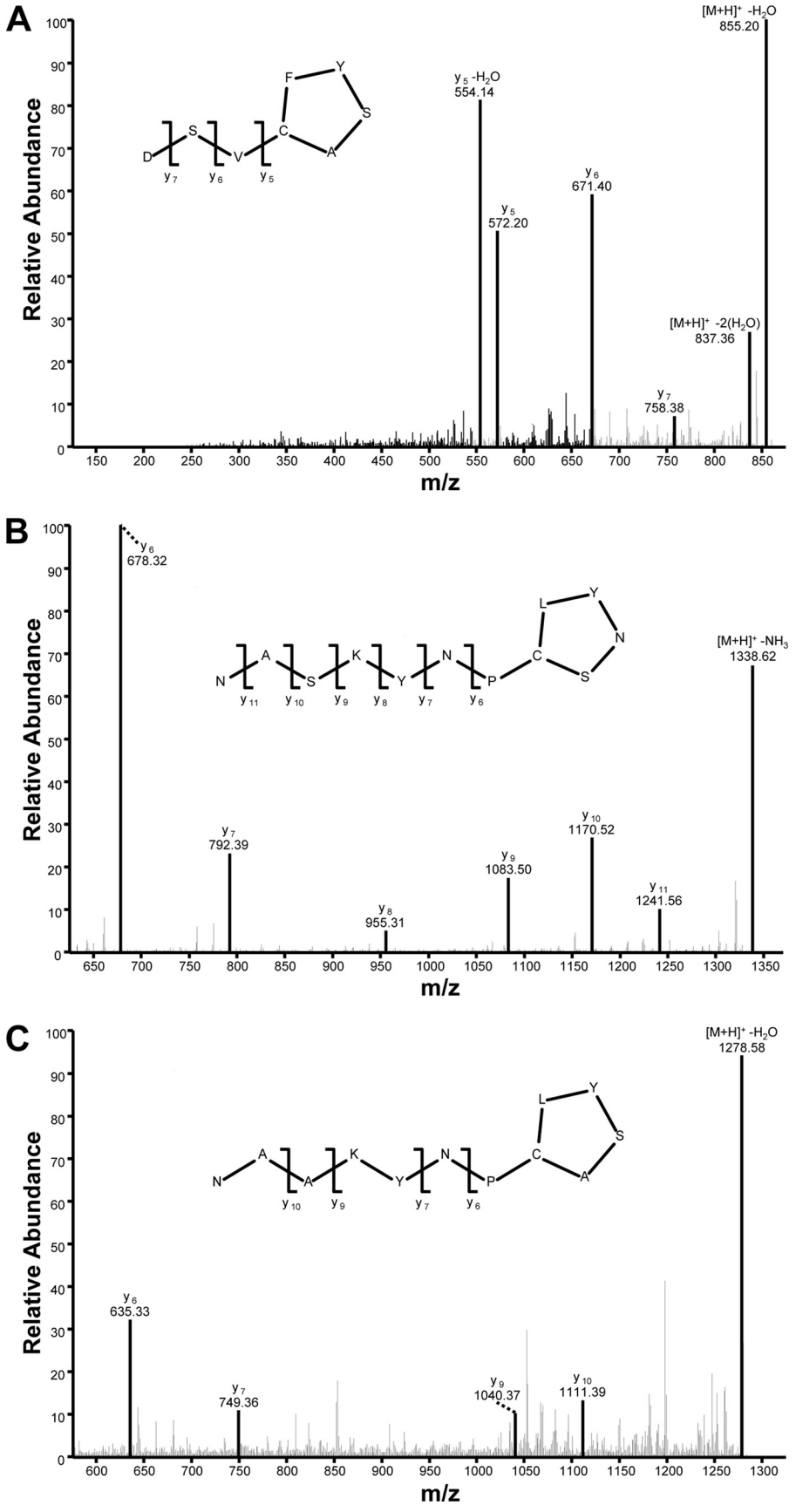

FIG 3 *S. epidermidis* AIP identification. This figure shows MS-MS spectra that result from collisionally induced dissociation of the $[M+H]^+$ ions for AIP-I (*m/z* 873.34) (A), AIP-2 (*m/z* 1,355.60) (B), and AIP-3 (*m/z* 1,296.60) (C). Predicted structures for all three AIPs and fragment assignments supporting these predictions are included.

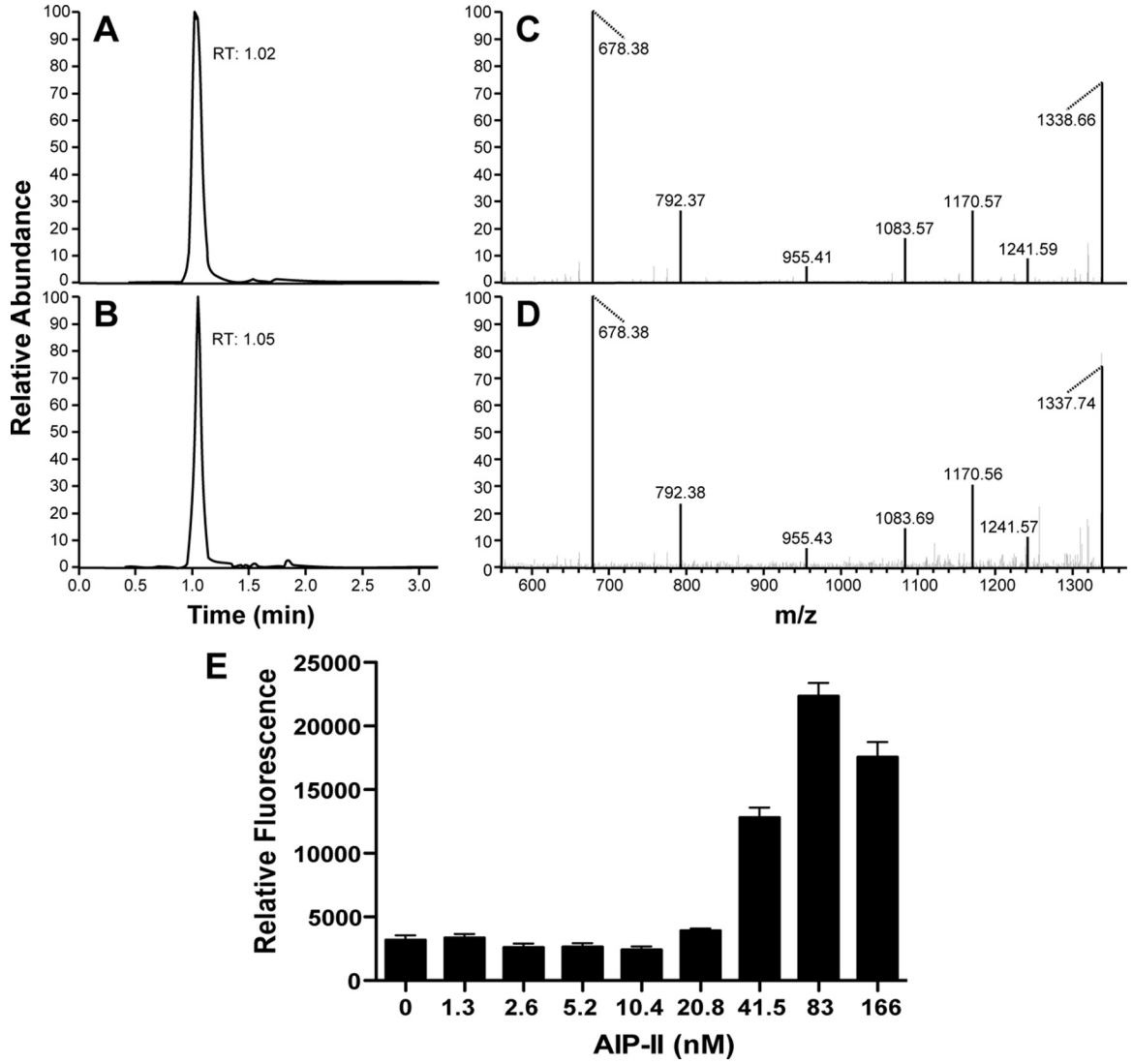

FIG 4 Confirmation of structure by comparison with synthetic AIP-II. Selected ion chromatograms for the fragment at *m/z* 678.33 obtained from collisionally induced dissociation of the $[M+H]^+$ ion at *m/z* 1,355.60 for both synthetic AIP-II (A) and spent medium from *S. epidermidis* strain 1457 (B). These chromatograms show excellent agreement in retention time (RT) between the two ions. As further confirmation, panels C and D demonstrate that the MS-MS spectrum for synthetic AIP-II (C) matches that of the putative AIP-II ion from *S. epidermidis* strain 1457. The MS-MS spectra were obtained by collisionally induced dissociation of a precursor ion at *m/z* 1,355.60 (the $[M+H]^+$ ion of AIP-II). (E) As a biological confirmation of the synthetic AIP-II, WT 1457 with the *agr* P_3-GFP reporter was grown with increasing doses of AIP-II, and absorbance and fluorescence readings were taken after 24 h. Relative fluorescence was plotted at the indicated AIP-II concentrations.

against the FRET substrate (Fig. 7A), demonstrating that no other proteases contributed to the activity measurements. To further assess the role of quorum-sensing regulation in Ecp regulation, spent-medium cross talk tests were performed using information gleaned from the results outlined in Fig. 5. For each *S. epidermidis* *agr* system, spent medium from that *agr* type added back to the same strain induced Ecp activity (Fig. 7B). In contrast, spent medium from a known interfering strain inhibited activity, resulting in significantly reduced Ecp activity. Taken together, these Ecp findings support the *agr* transcriptional reporter (Fig. 5) and microarray results (Fig. 6).

***S. epidermidis* colonizes pig skin in an *agr*-dependent manner.** We hypothesized that *S. epidermidis* retains the *agr* system because it facilitates successful colonization of the host. Using a previously developed skin colonization model (34), we compared the ability of WT 1457 and the Δ*rnaIII*::*dhfr* mutant to colonize freshly isolated porcine skin for 2 days. At this time point, a significant defect in the ability of the Δ*rnaIII*::*dhfr* mutant to colonize was observed (Fig. 8), indicating that *S. epidermidis* does require the *agr* system for optimal growth during skin colonization.

DISCUSSION

S. epidermidis is the most frequent cause of device-related infections (6). One of the important regulators that control the production of *S. epidermidis* virulence factors is the *agr* quorum-sensing system. Despite the significance of *agr*, key molecular details about this system have remained unknown, and in this work, we addressed some of these open questions. Using a mass spectrom-

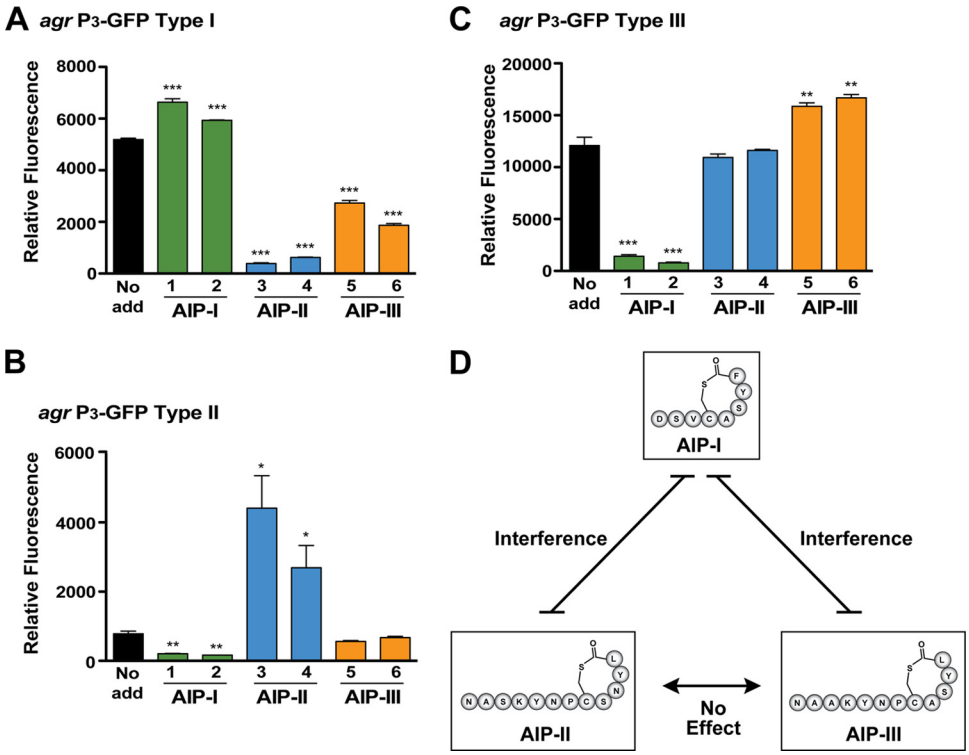

FIG 5 Identification of *agr* interference in *S. epidermidis*. Spent medium from *S. epidermidis* strains representing each *agr* type was collected and added to reporter strains to 10% of the total volume. The reporters were grown for 24 h, and GFP fluorescence was measured (***, $P < 0.001$, **, $P < 0.01$, and *, $P < 0.005$, relative to the no-addition reporter [no add], as determined by paired *t* test). (A) *agr* type I reporter. (B) *agr* type II reporter. (C) *agr* type III reporter. The strains used for spent medium addition were as follows: 1, ATCC 12228 (*agr* type I); 2, 7237 (*agr* type I); 3, 1457 (*agr* type II); 4, 5183 (*agr* type II); 5, 8247 (*agr* type III); 6, 8099 (type III). (D) Schematic of identified cross talk network between AIP-I, AIP-II, and AIP-III.

etry approach, we elucidated the structures of AIP-II and AIP-III and confirmed the previous deduction of AIP-I. We also discovered that *agr* interference occurs between the three *S. epidermidis agr* systems and, through transcriptional profiling, discovered striking regulation of the cysteine protease Ecp. Finally, we demonstrated that *S. epidermidis* retains the *agr* system for optimal skin colonization.

The mass spectrometry assignment of AIP-II and AIP-III indicated that both of these structures are 12 residues in length, making them the largest staphylococcal AIPs identified to date (14). The reason for this large AIP size is not clear. Both AIP sequences start on the C-terminal side of the highly conserved IG motif, which is found in most AgrD sequences (Fig. 1), and this junction could be important for release of AIP from the cytoplasmic membrane. The housekeeping type I signal peptidase is known to release *S. aureus* AIP-I in this manner (41), but it is possible that other resident proteases have this function among the staphylococci. Considering that the identical sequence is present at the *S. epidermidis* cleavage site in AgrD-II and AgrD-III (VIG ↓ NA), it seems likely that the same protease is responsible for the release. While this is not a typical type I signal peptidase cleavage site, these residues are in the allowed wobble for signal peptidase recognition (42). The AgrD-I cleavage site is also C-terminal to a similar sequence with a glycine residue (VAG ↓ DSV), and it may be that release of AIP is due to the same peptidase in these *S. epidermidis* strains.

Our mass spectrometry approach confirmed the structure of AIP-I. This structure was previously identified using a systematic approach that tested synthetic AIP-Is with various possible lengths of the N-terminal extension. Through process of elimination, it was determined that DSVCASYF was the most active; thus, it was inferred that it was the correct structure (16). In the present study, the AIP was purified from *agr* type I spent medium and demonstrated to have the identical structure (Fig. 3A). Using an alternative approach and medium collected directly from *S. epidermidis*, our analysis converged on the same structure, supporting the initial AIP-I report.

This is the first study to identify cross talk between the *S. epidermidis agr* systems. The phenomenon of *agr* interference was first identified in *S. aureus* and works as cross-inhibition between the *agr* type I, II, and III systems (37), while the similarities between type I and IV signals make them essentially interchangeable (14). By constructing *agr* reporters in each *S. epidermidis* system, we determined that *agr* interference also occurs in this species. There is strong interference between the *agr* type I and II systems and between the type I and III systems (Fig. 5). In some studies, the type I strains were the most frequently identified in *S. epidermidis* infections (19, 21, 22), and perhaps these interference properties give these strains a competitive advantage. However, the high prevalence of *agr* type I strains is not universal, as a recent large study of 200 *S. epidermidis* isolates from hospitalized patients in Germany found over two-thirds to be *agr* type II and III (23).

We did not observe interference between the *agr* type II and III systems. Although these signals are similar, they do not significantly cross-activate the *agr* type III and type II systems, respectively (Fig. 5D). The reason for this is not clear, but it is known that

A

Gene description	Gene name	Locus tag	Fold downregulated
delta-hemolysin	*hld*	SE1634	49.6
phenol soluble modulin β1/β2	*psm β1b*	SE0849	25.7
Staphopain cysteine proteinase	*ecp*	SE0184	19.1
phenol soluble modulin β1/β2	*psm β1a*	SE0848	16.6
accessory gene regulator C	*agrC*	SE1637	4.8
glycerol ester hydrolase	*geh*	SE0185	3.8
succinyl-diaminopimelate desuccinylase		SE0216	3.7
PTS system sucrose-specific IIBC component		SE1890	3.6
accessory gene regulator A	*agrA*	SE1638	3.4
transmembrane efflux pump protein		SE0196	3.4
acetoin(diacetyl)reductase		SE2225	3.1
putative NADH-dependent flavin oxidoreductase		SE0195	3.1
formate acetyltransferase activating enzyme	*pflA*	SE0215	2.8
transcription regulator GntR family		SE1625	2.6
nickel ABC transporter nickel-binding protein		SE1981	2.4
formate acetyltransferase	*pflB*	SE0214	2.4
ABC transporter (ATP-binding protein)		SE1624	2.3
acetoin(diacetyl)reductase	*butA*	SE0197	2.2
transcription regulator RpiR family		SE1891	2.1

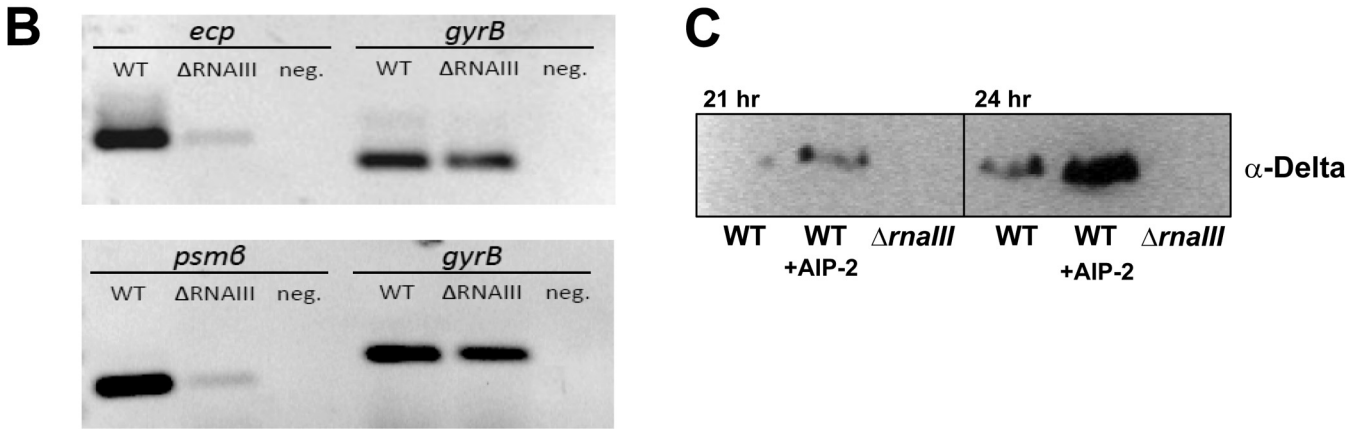

FIG 6 Transcriptional profiling of *S. epidermidis* Δ*rnaIII* mutant. (A) Heat map of the microarray results of WT 1457 versus the Δ*rnaIII* mutant. (B) RT-PCR results of the WT versus the Δ*rnaIII* mutant for PSMβ and *ecp* genes, along with *gyrB* as a control. (C) Protein immunoblot of δ-toxin in WT 1457 and the Δ*rnaIII* mutant. The addition of AIP-II (40 nM) induces δ-toxin expression.

signal activation is more difficult to achieve than inhibition in staphylococcal *agr* systems (14). With an activating signal, there is specificity built into the AgrC receptor for proper interactions with the AIP structure to initiate the cascade, and the few residue differences between these *S. epidermidis* AIP-II and AIP-III signals may contain the necessary structural information for activation. With this lack of both cross-activation and inhibition, the AgrC receptor in a type II strain is essentially signal blind to AIP-III, and a similar conclusion could be made for AgrC type III interacting with AIP-II. Thus, the only significant *S. epidermidis* cross talk is between the *agr* type I and II/III systems.

Given that colonization and biofilm formation are key aspects of *S. epidermidis* pathogenesis, it is surprising that some reports indicate that *agr*-defective strains are better biofilm formers (9, 43) and adhere more effectively to human skin epithelia (43). However, time course studies indicate that *agr* is necessary in certain biofilm developmental stages (12), and our findings indicate that *agr* is necessary for optimal skin colonization (Fig. 8), suggesting that the contributions of the *agr* system are likely more important than originally projected. In part, this could be due to the fact that proteases are important for processing the accumulation-associated protein (Aap) (8). Aap is a critical player in aspects of *S. epidermidis* biofilm development, but the expression of this protein appears to be *agr* independent. The study reported here and others (11, 12) demonstrate that proteases are under *agr* quorum-sensing control, and it is possible that these proteases modulate biofilm structure in some capacity. Of the major extracellular proteases produced, Esp protease was found to be important in polymicrobial interactions with *S. aureus* (44), demonstrating that *S. epidermidis* needs to produce extracellular proteases to effectively compete during colonization. The importance of the *S. epidermidis agr* system in evasion of innate immunity has also been demonstrated (11), and the metalloprotease SepA was shown to inactivate the antimicrobial peptide dermcidin (45). Taken together, these observations highlight a clear need for pathogenic *S. epidermidis* strains to retain an active *agr* system, which would make quorum sensing inhibition through *agr* interference an effective competition strategy. This could explain in part the evolution of intraspecies quorum-sensing inhibition that we identified in this study (Fig. 5). The *S. aureus agr* system is a prime target for

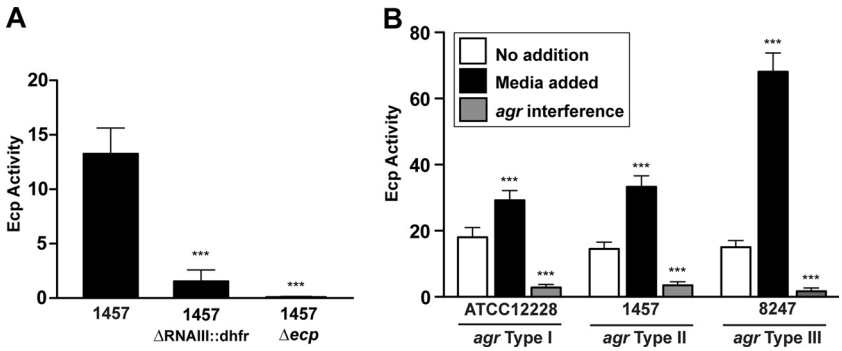

FIG 7 Quorum-sensing control of Ecp protease activity. (A) Ecp activity in spent medium collected from WT 1457 and strains with Δ*rnaIII*::*dhfr* or Δ*ecp* mutations. Activity was measured by FRET substrate (***, $P < 0.001$ relative to WT 1457, as determined by paired *t* test). (B) *S. epidermidis* strains representing *agr* type I (ATCC 12228), type II (1457), and type III (8247) were grown without addition or in the presence of inducing spent medium (medium added) or inhibiting spent medium (*agr* interference; 1457 for type I, 12228 for type II or III). Ecp activity was measured and plotted (***, $P < 0.001$ relative to no addition, as determined by paired *t* test).

development of antivirulence therapeutics (46–48), and a similar strategy could be applied to *S. epidermidis*.

Our regulation studies revealed that the cysteine protease Ecp is one of the most highly regulated factors under the control of the *S. epidermidis agr* system. In support of this observation, expression of the *ecp* gene was observed in a previous array study (11). Surprisingly, our microarray analyses did not reveal regulation of the serine protease Esp or the metalloprotease SepA, although there are previous reports that these enzymes are *agr* regulated (11, 12). The reason for these differences are not clear and could be due to the nature of the *agr* mutations used or to strain-dependent variances. In this study, only the RNAIII transcript was disrupted, while in other studies, complete *agr* deletions were used. Interestingly, the Ecp homolog in *S. aureus*, staphopain A, was recently shown to have a dramatic impact on biofilm structure (39), suggesting that the effect Ecp has on *S. epidermidis* biofilms warrants further investigation.

The knowledge gained from our study will aid interpretation of results from reported and ongoing investigations. For instance, cross talk between staphylococci has been observed in the nasal colonization environment (44, 49), and the availability of AIP structural information and defined interference patterns could improve our understanding of these observations. In terms of treatment approaches, it is known that a functional *agr* system is important for hematogenous spread of *S. epidermidis* in device infections (13), and the addition of synthetic AIPs could be used to modulate these phenotypes in a manner similar to those used in previous *S. aureus* studies (50, 51). While *S. epidermidis* and other CoNS do not garner as much attention as *S. aureus*, the clinical burden of these infections is significant, and this new information on the *S. epidermidis agr* system provides important insights for future studies.

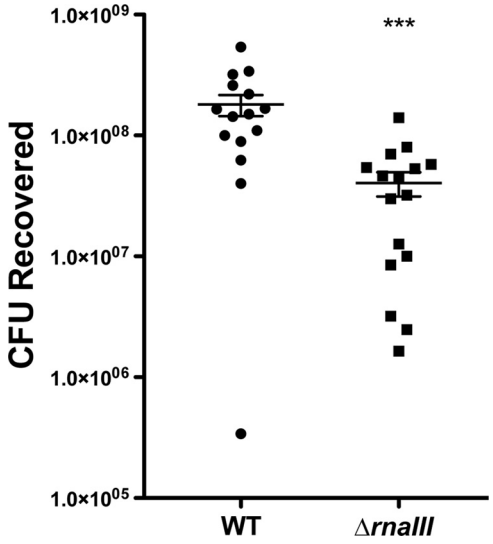

FIG 8 *S. epidermidis agr* is required for optimal skin colonization. WT 1457 and 1457 Δ*rnaIII*::*dhfr* were cultured on pig skin biopsy specimens for 48 h. Recovered CFU were enumerated, and the values were plotted as means and standard errors of the means (***, $P < 0.001$).

ACKNOWLEDGMENTS

We thank C. Malone for technical assistance and D. Stoltz for proving porcine skin tissue.

This work was funded in part by NIH public health service grants AI049311 to P.D.F. and AI083211 (Project 3) to A.R.H. Mass spectrometry data were collected in the Triad Mass Spectrometry Facility at the University of North Carolina Greensboro.

REFERENCES

1. **Otto M.** 2009. *Staphylococcus epidermidis*—the 'accidental' pathogen. Nat. Rev. Microbiol. **7**:555–567. http://dx.doi.org/10.1038/nrmicro2182.
2. **Hidron AI, Edwards JR, Patel J, Horan TC, Sievert DM, Pollock DA, Fridkin SK.** 2008. NHSN annual update: antimicrobial-resistant pathogens associated with healthcare-associated infections: annual summary of data reported to the National Healthcare Safety Network at the Centers for Disease Control and Prevention, 2006–2007. Infect. Control Hosp. Epidemiol. **29**:996–1011. http://dx.doi.org/10.1086/591861.
3. **Murdoch DR, Corey GR, Hoen B, Miro JM, Fowler VG, Jr, Bayer AS, Karchmer AW, Olaison L, Pappas PA, Moreillon P, Chambers ST, Chu VH, Falco V, Holland DJ, Jones P, Klein JL, Raymond NJ, Read KM, Tripodi MF, Utili R, Wang A, Woods CW, Cabell CH.** 2009. Clinical presentation, etiology, and outcome of infective endocarditis in the 21st century: the International Collaboration on Endocarditis-Prospective Cohort Study. Arch. Intern. Med. **169**:463–473. http://dx.doi.org/10.1001/archinternmed.2008.603.
4. **Mermel LA, Allon M, Bouza E, Craven DE, Flynn P, O'Grady NP, Raad II, Rijnders BJ, Sherertz RJ, Warren DK.** 2009. Clinical practice guidelines for the diagnosis and management of intravascular catheter-related infection: 2009 update by the Infectious Diseases Society of America. Clin. Infect. Dis. **49**:1–45. http://dx.doi.org/10.1086/599376.
5. **Darouiche RO.** 2001. Device-associated infections: a macroproblem that

starts with microadherence. Clin. Infect. Dis. **33:**1567–1572. http://dx.doi.org/10.1086/323130.
6. **Mack D, Davies AP, Harris LG, Jeeves R, Pascoe B, Knobloch JK, Rohde H, Wilkinson TS.** 2013. *Staphylococcus epidermidis* in biomaterial-associated infections, p 25–56. *In* Moriarty F, Zaat SAJ, Busscher H (ed), Biomaterials associated infection: immunological aspects and antimicrobial strategies. Springer, New York, NY.
7. **Heilmann C, Schweitzer O, Gerke C, Vanittanakom N, Mack D, Gotz F.** 1996. Molecular basis of intercellular adhesion in the biofilm-forming *Staphylococcus epidermidis*. Mol. Microbiol. **20:**1083–1091. http://dx.doi.org/10.1111/j.1365-2958.1996.tb02548.x.
8. **Rohde H, Burdelski C, Bartscht K, Hussain M, Buck F, Horstkotte MA, Knobloch JK, Heilmann C, Herrmann M, Mack D.** 2005. Induction of *Staphylococcus epidermidis* biofilm formation via proteolytic processing of the accumulation-associated protein by staphylococcal and host proteases. Mol. Microbiol. **55:**1883–1895. http://dx.doi.org/10.1111/j.1365-2958.2005.04515.x.
9. **Vuong C, Gerke C, Somerville GA, Fischer ER, Otto M.** 2003. Quorum-sensing control of biofilm factors in *Staphylococcus epidermidis*. J. Infect. Dis. **188:**706–718. http://dx.doi.org/10.1086/377239.
10. **Vuong C, Gotz F, Otto M.** 2000. Construction and characterization of an *agr* deletion mutant of *Staphylococcus epidermidis*. Infect. Immun. **68:**1048–1053. http://dx.doi.org/10.1128/IAI.68.3.1048-1053.2000.
11. **Yao Y, Vuong C, Kocianova S, Villaruz AE, Lai Y, Sturdevant DE, Otto M.** 2006. Characterization of the *Staphylococcus epidermidis* accessory-gene regulator response: quorum-sensing regulation of resistance to human innate host defense. J. Infect. Dis. **193:**841–848. http://dx.doi.org/10.1086/500246.
12. **Batzilla CF, Rachid S, Engelmann S, Hecker M, Hacker J, Ziebuhr W.** 2006. Impact of the accessory gene regulatory system (Agr) on extracellular proteins, *codY* expression and amino acid metabolism in *Staphylococcus epidermidis*. Proteomics **6:**3602–3613. http://dx.doi.org/10.1002/pmic.200500732.
13. **Wang R, Khan BA, Cheung GY, Bach TH, Jameson-Lee M, Kong KF, Queck SY, Otto M.** 2011. *Staphylococcus epidermidis* surfactant peptides promote biofilm maturation and dissemination of biofilm-associated infection in mice. J. Clin. Invest. **121:**238–248. http://dx.doi.org/10.1172/JCI42520.
14. **Thoendel M, Kavanaugh JS, Flack CE, Horswill AR.** 2011. Peptide signaling in the staphylococci. Chem. Rev. **111:**117–151. http://dx.doi.org/10.1021/cr100370n.
15. **Novick RP, Geisinger E.** 2008. Quorum sensing in staphylococci. Annu. Rev. Genet. **42:**541–564. http://dx.doi.org/10.1146/annurev.genet.42.110807.091640.
16. **Otto M, Sussmuth R, Jung G, Gotz F.** 1998. Structure of the pheromone peptide of the *Staphylococcus epidermidis agr* system. FEBS Lett. **424:**89–94. http://dx.doi.org/10.1016/S0014-5793(98)00145-8.
17. **Van Wamel WJ, van Rossum G, Verhoef J, Vandenbroucke-Grauls CM, Fluit AC.** 1998. Cloning and characterization of an accessory gene regulator (*agr*)-like locus from *Staphylococcus epidermidis*. FEMS Microbiol. Lett. **163:**1–9. http://dx.doi.org/10.1111/j.1574-6968.1998.tb13018.x.
18. **Dufour P, Jarraud S, Vandenesch F, Greenland T, Novick RP, Bes M, Etienne J, Lina G.** 2002. High genetic variability of the *agr* locus in *Staphylococcus* species. J. Bacteriol. **184:**1180–1186. http://dx.doi.org/10.1128/jb.184.4.1180-1186.2002.
19. **Carmody AB, Otto M.** 2004. Specificity grouping of the accessory gene regulator quorum-sensing system of *Staphylococcus epidermidis* is linked to infection. Arch. Microbiol. **181:**250–253. http://dx.doi.org/10.1007/s00203-003-0644-2.
20. **Rosenthal ME, Dever LL, Moucha CS, Chavda KD, Otto M, Kreiswirth BN.** 2011. Molecular characterization of an early invasive *Staphylococcus epidermidis* prosthetic joint infection. Microb. Drug Resist. **17:**345–350. http://dx.doi.org/10.1089/mdr.2010.0157.
21. **Li M, Guan M, Jiang XF, Yuan FY, Xu M, Zhang WZ, Lu Y.** 2004. Genetic polymorphism of the accessory gene regulator (*agr*) locus in *Staphylococcus epidermidis* and its association with pathogenicity. J. Med. Microbiol. **53:**545–549. http://dx.doi.org/10.1099/jmm.0.05406-0.
22. **Hellmark B, Soderquist B, Unemo M, Nilsdotter-Augustinsson A.** 2013. Comparison of *Staphylococcus epidermidis* isolated from prosthetic joint infections and commensal isolates in regard to antibiotic susceptibility, *agr* type, biofilm production, and epidemiology. Int. J. Med. Microbiol. **303:**32–39. http://dx.doi.org/10.1016/j.ijmm.2012.11.001.
23. **Mertens A, Ghebremedhin B.** 2013. Genetic determinants and biofilm formation of clinical *Staphylococcus epidermidis* isolates from blood cultures and indwelling devises. Eur. J. Microbiol. Immunol. **3:**111–119. http://dx.doi.org/10.1556/EuJMI.3.2013.2.4.
24. **Nair D, Memmi G, Hernandez D, Bard J, Beaume M, Gill S, Francois P, Cheung AL.** 2011. Whole-genome sequencing of *Staphylococcus aureus* strain RN4220, a key laboratory strain used in virulence research, identifies mutations that affect not only virulence factors but also the fitness of the strain. J. Bacteriol. **193:**2332–2335. http://dx.doi.org/10.1128/JB.00027-11.
25. **Maliszewski KL, Nuxoll AS.** 2014. Use of electroporation and conjugative mobilization for genetic manipulation of *Staphylococcus epidermidis*. Methods Mol. Biol. **1106:**125–134. http://dx.doi.org/10.1007/978-1-62703-736-5_11.
26. **Olson ME, Horswill AR.** 2014. Bacteriophage transduction in *Staphylococcus epidermidis*. Methods Mol. Biol. **1106:**167–172. http://dx.doi.org/10.1007/978-1-62703-736-5_15.
27. **Handke LD, Slater SR, Conlon KM, O'Donnell ST, Olson ME, Bryant KA, Rupp ME, O'Gara JP, Fey PD.** 2007. SigmaB and SarA independently regulate polysaccharide intercellular adhesin production in *Staphylococcus epidermidis*. Can. J. Microbiol. **53:**82–91. http://dx.doi.org/10.1139/w06-108.
28. **Projan SJ, Archer GL.** 1989. Mobilization of the relaxable *Staphylococcus aureus* plasmid pC221 by the conjugative plasmid pGO1 involves three pC221 loci. J. Bacteriol. **171:**1841–1845.
29. **Mack D, Rohde H, Dobinsky S, Riedewald J, Nedelmann M, Knobloch JK, Elsner HA, Feucht HH.** 2000. Identification of three essential regulatory gene loci governing expression of *Staphylococcus epidermidis* polysaccharide intercellular adhesin and biofilm formation. Infect. Immun. **68:**3799–3807. http://dx.doi.org/10.1128/IAI.68.7.3799-3807.2000.
30. **Bae T, Schneewind O.** 2006. Allelic replacement in *Staphylococcus aureus* with inducible counter-selection. Plasmid **55:**58–63. http://dx.doi.org/10.1016/j.plasmid.2005.05.005.
31. **Beenken KE, Dunman PM, McAleese F, Macapagal D, Murphy E, Projan SJ, Blevins JS, Smeltzer MS.** 2004. Global gene expression in *Staphylococcus aureus* biofilms. J. Bacteriol. **186:**4665–4684. http://dx.doi.org/10.1128/JB.186.14.4665-4684.2004.
32. **Kiedrowski MR, Kavanaugh JS, Malone CL, Mootz JM, Voyich JM, Smeltzer MS, Bayles KW, Horswill AR.** 2011. Nuclease modulates biofilm formation in community-associated methicillin-resistant *Staphylococcus aureus*. PLoS One **6:**e26714. http://dx.doi.org/10.1371/journal.pone.0026714.
33. **Laarman AJ, Mijnheer G, Mootz JM, van Rooijen WJ, Ruyken M, Malone CL, Heezius EC, Ward R, Milligan G, van Strijp JA, de Haas CJ, Horswill AR, van Kessel KP, Rooijakkers SH.** 2012. *Staphylococcus aureus* staphopain A inhibits CXCR2-dependent neutrophil activation and chemotaxis. EMBO J. **31:**3607–3619. http://dx.doi.org/10.1038/emboj.2012.212.
34. **Ohnemus U, Kohrmeyer K, Houdek P, Rohde H, Wladykowski E, Vidal S, Horstkotte MA, Aepfelbacher M, Kirschner N, Behne MJ, Moll I, Brandner JM.** 2008. Regulation of epidermal tight-junctions (TJ) during infection with exfoliative toxin-negative *Staphylococcus* strains. J. Investig. Dermatol. **128:**906–916. http://dx.doi.org/10.1038/sj.jid.5701070.
35. **Moll I, Houdek P, Schmidt H, Moll R.** 1998. Characterization of epidermal wound healing in a human skin organ culture model: acceleration by transplanted keratinocytes. J. Investig. Dermatol. **111:**251–258. http://dx.doi.org/10.1046/j.1523-1747.1998.00265.x.
36. **Malone CL, Boles BR, Lauderdale KJ, Thoendel M, Kavanaugh JS, Horswill AR.** 2009. Fluorescent reporters for *Staphylococcus aureus*. J. Microbiol. Methods **77:**251–260. http://dx.doi.org/10.1016/j.mimet.2009.02.011.
37. **Ji G, Beavis R, Novick RP.** 1997. Bacterial interference caused by autoinducing peptide variants. Science **276:**2027–2030. http://dx.doi.org/10.1126/science.276.5321.2027.
38. **Malone CL, Boles BR, Horswill AR.** 2007. Biosynthesis of *Staphylococcus aureus* autoinducing peptides by using the synechocystis DnaB mini-intein. Appl. Environ. Microbiol. **73:**6036–6044. http://dx.doi.org/10.1128/AEM.00912-07.
39. **Mootz JM, Malone CL, Shaw LN, Horswill AR.** 2013. Staphopains modulate *Staphylococcus aureus* biofilm integrity. Infect. Immun. **81:**3227–3238. http://dx.doi.org/10.1128/IAI.00377-13.
40. **Dubin G, Chmiel D, Mak P, Rakwalska M, Rzychon M, Dubin A.** 2001. Molecular cloning and biochemical characterisation of proteases from *Staphylococcus epidermidis*. Biol. Chem. **382:**1575–1582.

41. **Kavanaugh JS, Thoendel M, Horswill AR.** 2007. A role for type I signal peptidase in *Staphylococcus aureus* quorum sensing. Mol. Microbiol. **65:** 780–798. http://dx.doi.org/10.1111/j.1365-2958.2007.05830.x.
42. **Paetzel M, Karla A, Strynadka NC, Dalbey RE.** 2002. Signal peptidases. Chem. Rev. **102:**4549–4580. http://dx.doi.org/10.1021/cr010166y.
43. **Vuong C, Kocianova S, Yao Y, Carmody AB, Otto M.** 2004. Increased colonization of indwelling medical devices by quorum-sensing mutants of *Staphylococcus epidermidis* in vivo. J. Infect. Dis. **190:**1498–1505. http://dx.doi.org/10.1086/424487.
44. **Iwase T, Uehara Y, Shinji H, Tajima A, Seo H, Takada K, Agata T, Mizunoe Y.** 2010. *Staphylococcus epidermidis* Esp inhibits *Staphylococcus aureus* biofilm formation and nasal colonization. Nature **465:**346–349. http://dx.doi.org/10.1038/nature09074.
45. **Lai Y, Villaruz AE, Li M, Cha DJ, Sturdevant DE, Otto M.** 2007. The human anionic antimicrobial peptide dermcidin induces proteolytic defence mechanisms in staphylococci. Mol. Microbiol. **63:**497–506. http://dx.doi.org/10.1111/j.1365-2958.2006.05540.x.
46. **Cech NB, Horswill AR.** 2013. Small-molecule quorum quenchers to prevent *Staphylococcus aureus* infection. Future Microbiol. **8:**1511–1514. http://dx.doi.org/10.2217/fmb.13.134.
47. **Gordon CP, Williams P, Chan WC.** 2013. Attenuating *Staphylococcus aureus* virulence gene regulation: a medicinal chemistry perspective. J. Med. Chem. **56:**1389–1404. http://dx.doi.org/10.1021/jm3014635.
48. **Gray B, Hall P, Gresham H.** 2013. Targeting *agr*- and *agr*-like quorum sensing systems for development of common therapeutics to treat multiple gram-positive bacterial infections. Sensors (Basel) **13:**5130–5166. http://dx.doi.org/10.3390/s130405130.
49. **Lina G, Boutite F, Tristan A, Bes M, Etienne J, Vandenesch F.** 2003. Bacterial competition for human nasal cavity colonization: role of Staphylococcal *agr* alleles. Appl. Environ. Microbiol. **69:**18–23. http://dx.doi.org/10.1128/AEM.69.1.18-23.2003.
50. **Lauderdale KJ, Malone CL, Boles BR, Morcuende J, Horswill AR.** 2010. Biofilm dispersal of community-associated methicillin-resistant *Staphylococcus aureus* on orthopedic implant material. J. Orthop. Res. **28:**55–61. http://dx.doi.org/10.1002/jor.20943.
51. **Boles BR, Horswill AR.** 2008. *agr*-mediated dispersal of *Staphylococcus aureus* biofilms. PLoS Pathog. **4:**e1000052. http://dx.doi.org/10.1371/journal.ppat.1000052.
52. **Boles BR, Thoendel M, Roth AJ, Horswill AR.** 2010. Identification of genes involved in polysaccharide-independent *Staphylococcus aureus* biofilm formation. PLoS One **5:**e10146. http://dx.doi.org/10.1371/journal.pone.0010146.
53. **Zhang YQ, Ren SX, Li HL, Wang YX, Fu G, Yang J, Qin ZQ, Miao YG, Wang WY, Chen RS, Shen Y, Chen Z, Yuan ZH, Zhao GP, Qu D, Danchin A, Wen YM.** 2003. Genome-based analysis of virulence genes in a non-biofilm-forming *Staphylococcus epidermidis* strain (ATCC 12228). Mol. Microbiol. **49:**1577–1593. http://dx.doi.org/10.1046/j.1365-2958.2003.03671.x.
54. **Mack D, Siemssen N, Laufs R.** 1992. Parallel induction by glucose of adherence and a polysaccharide antigen specific for plastic-adherent *Staphylococcus epidermidis*: evidence for functional relation to intercellular adhesion. Infect. Immun. **60:**2048–2057.
55. **Gill SR, Fouts DE, Archer GL, Mongodin EF, Deboy RT, Ravel J, Paulsen IT, Kolonay JF, Brinkac L, Beanan M, Dodson RJ, Daugherty SC, Madupu R, Angiuoli SV, Durkin AS, Haft DH, Vamathevan J, Khouri H, Utterback T, Lee C, Dimitrov G, Jiang L, Qin H, Weidman J, Tran K, Kang K, Hance IR, Nelson KE, Fraser CM.** 2005. Insights on evolution of virulence and resistance from the complete genome analysis of an early methicillin-resistant *Staphylococcus aureus* strain and a biofilm-producing methicillin-resistant *Staphylococcus epidermidis* strain. J. Bacteriol. **187:**2426–2438. http://dx.doi.org/10.1128/JB.187.7.2426-2438.2005.